

EVALUATION OF ZINC-BASED ALLOY FOR SLM 3D PRINTING

Kristína KOVALČÍKOVÁ, Dominik DUBEC, Marek ŠOLC

Institute of Metallurgical Technologies and Digital Transformation, Faculty of Materials, Metallurgy and Recycling, Technical University of Kosice, Kosice, Slovakia, kristina.kovalcikova@tuke.sk

https://doi.org/10.37904/metal.2025.5095

Abstract

This study investigates the feasibility of processing the Zn0.4Mg0.4Ca alloy using Selective Laser Melting (SLM) for potential application in biodegradable medical implants. As part of the initial phase of a broader research effort, five test samples were successfully printed and subjected to basic material characterization. Microhardness measurements yielded an average of 115.2 HV1, significantly exceeding the hardness of pure zinc, indicating the strengthening effect of the alloying elements. Surface roughness analysis revealed significant anisotropy, with Ra values of 10.76 µm parallel and 25.69 µm perpendicular to the build layers, underscoring the need for additional surface post-processing. The measured density was high and slightly exceeded theoretical expectations, indicating excellent structural compaction and low porosity. These findings confirm the alloy's printability and provide a solid foundation for future research focused on printing and evaluating specific implant geometries, including mechanical, microstructural, and biocompatibility assessments.

Keywords: Biodegradable implants, zinc alloy, selective laser melting additive technology

1. INTRODUCTION

Biodegradable metals represent a promising class of materials for temporary implants that are gradually resorbed by the body, thus eliminating the need for secondary surgeries for implant removal. Zinc and its alloys have recently emerged as particularly attractive candidates due to their favorable corrosion rates, absence of gas release during degradation, and excellent biocompatibility [1,2]. Compared to magnesium- or iron-based biodegradable implants, zinc alloys offer a balanced combination of sufficient mechanical strength, appropriate degradation kinetics, and metabolic safety regarding Zn²⁺ ion release [1,3].

The alloying of zinc with elements such as magnesium and calcium further enhances its mechanical performance and promotes bone tissue regeneration [4,5]. Magnesium notably improves the strength and ductility of the alloy [6], while calcium fosters osteointegration [5]. The Zn0.4Mg0.4Ca composition appears particularly well-suited to meet the mechanical and biological requirements for challenging orthopedic applications [9].

Selective Laser Melting (SLM) has emerged as a cutting-edge additive manufacturing technology, enabling the production of complex metallic implants directly from powder materials. The application of SLM for processing zinc and its alloys remains relatively unexplored but shows promising potential for biomedical use.

The Zn0.4Mg0.4Ca alloy was initially prepared by melting and gravity casting of pure elemental constituents under a protective argon atmosphere, followed by thermomechanical processing via hot extrusion. Mechanical testing of the extruded material confirmed that zinc-based alloys exhibit sufficient strength to withstand physiological loading conditions, with mechanical properties falling between those of pure magnesium and titanium. Importantly, the mechanical behavior of this alloy closely approximates that of natural bone tissue, thereby improving implant integration while minimizing the risk of stress shielding. Furthermore, previous in



vitro studies have demonstrated the non-cytotoxic character of the Zn0.4Mg0.4Ca alloy, underscoring its promising potential for safe biomedical applications [9].

2. MATERIALS AND METHODS

In this study, five test specimens (**Figure 1 (a)**) with dimensions of $10 \times 5 \times 5$ mm were fabricated using a Dentas LMP 100 Arrow Metal system operating on the Selective Laser Melting (SLM) principle. The feedstock material was the Zn0.4Mg0.4Ca alloy, selected to evaluate its printability using SLM and to characterize the fundamental properties of the printed parts, namely microhardness, density and surface roughness. The powder morphology and particle size distribution met the standard requirements for SLM processing. The powder was atomized using ultrasonic vibrations, where a niobium plate oscillating at 40 Hz dispersed the molten metal into fine droplets and exhibited a spherical shape with particle sizes ranging from 15 to 85 μ m, with the majority falling between 30 and 60 μ m. **Figure 1(b)** shows a scanning electron microscope (SEM) image of the powder particles captured using a VEGA3 TESCAN instrument.

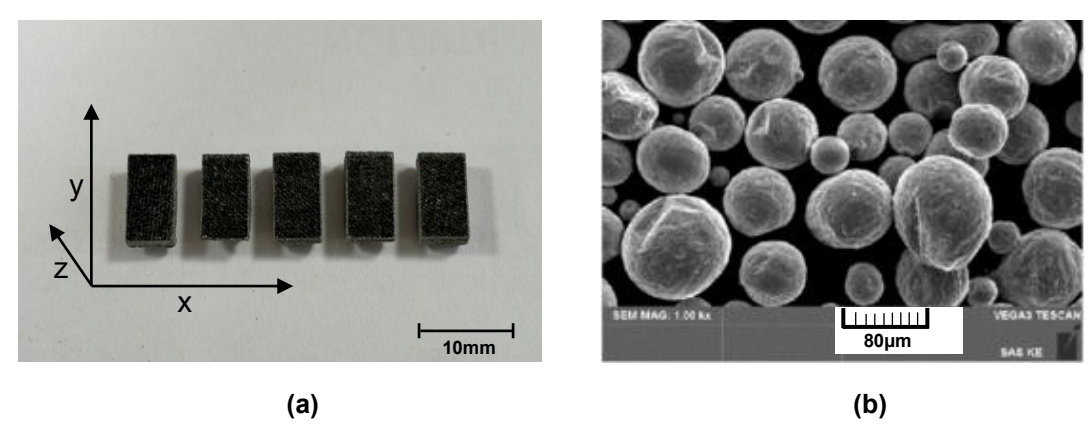


Figure 1 Printed samples using SLM technology (a), SEM of the particles (b) [9]

The fabrication process was carried out in an inert atmosphere with an oxygen concentration below 0.1 %. The printing system was equipped with an internal gas circulation unit to ensure proper filtering of metallic vapors generated during melting. Process parameters were optimized based on preliminary test prints. The layer thickness was set to 25 µm, corresponding to approximately 200 layers for a sample height of 5 mm. Laser power was set to 50 W, scanning speed to 500 mm/s, hatch spacing to 70 µm and scanning strategy was linear. The samples were built layer by layer along the z-axis, from bottom to top, as indicated in the coordinate system shown in **Figure 1 (a)**. A steel build plate was used for printing and was continuously heated throughout the entire process. The total print time for all the samples was approximately one hour.

The microhardness of the printed samples was measured using a 432 SVD hardness tester in accordance with the Vickers method (HV1), applying a load of 1 kgf for 10 seconds. Ten indentations were made at different locations on each sample to ensure more representative and objective results. Prior to testing, the sample was embedded in Polycast resin and subsequently ground using silicon carbide papers of grit sizes 320 to 1200. Final polishing was performed on an automatic polishing unit (TEGRAMIN 30) using diamond suspensions with particle sizes of 9, 3, and 1 μ m.

Surface roughness was measured on the side face of the printed specimen in two orientations: parallel and perpendicular to the layer deposition direction. As expected, the measured values differed between the two directions. This reflects the nature of the additive manufacturing process, where layer orientation influences surface texture depending on the measurement direction.

In addition to line roughness, areal surface roughness was also assessed, with deviation visualized through a deviation-color surface map. All measurements were performed using a Sensofar PLu Neox optical profilometer.



The density of the sample was determined using a gas pycnometer AccuPyc II 1340 (Micromeritics), which operates based on Boyle's law. The instrument calculates the volume of a solid object by measuring pressure changes of an inert gas (in this case, helium) within sealed reference and sample chambers. The measurement was conducted at a laboratory temperature of approximately 21 °C. From the change in helium pressure, the sample volume was automatically calculated, and in combination with the precisely known mass, the density was derived. The measurement was carried out over 10 cycles, preceded by 10 purge cycles to ensure system cleanliness. This method enables accurate determination of the true volume of the sample, independent of surface roughness or internal porosity.

3. RESULTS AND DISCUSSION

In **Table 1**, the averaged Vickers microhardness values (HV1) are presented along with the corresponding standard deviation. The average diagonal lengths of the indents were 128.44 μ m in the x-direction and 125.54 μ m in the y-direction.

Table 1 Summary of Vickers microhardness (HV1) measurements

Method	Hardness (HV1)	Standard deviation		
HV1	115.2	3.85		

The relatively high hardness of the Zn0.4Mg0.4Ca alloy sample can be largely attributed to the presence of alloying elements. A study focusing on the properties of biodegradable zinc-based alloys (Zn–Mg–Ca) reports that the addition of 1 % Mg and 1 % Ca can increase the hardness of hot-rolled pure zinc from 39 HV to 107 HV [1]. The presence of these elements also promotes the formation of intermetallic phases such as Mg₂Zn₁₁ and CaZn₁₃, which significantly contribute to the strengthening of the alloy matrix, as demonstrated in a study on mechanically alloyed Zn–Mg systems [10]. The selective laser melting process additionally induces rapid solidification, leading to grain refinement and the development of a more homogeneous microstructure, which further enhances the hardness of the material [7].

Profile roughness measurements were carried out in accordance with ISO 4287, in two orientations: parallel and perpendicular to the layer-building direction. The roughness values measured parallel to the layers are presented in **Table 2**, with the corresponding profile graph shown in **Figure 2**. The results obtained perpendicular to the layers are summarized in **Table 3**, and the related graph is shown in **Figure 3**. In addition, areal surface roughness was evaluated according to ISO 25178, with numerical values presented in **Table 4** and a 3D visualization of surface deviations displayed in **Figure 4**.

Table 2 Surface roughness parameters (ISO 4287) measured parallel to the layer orientation

<i>Rp</i>	Rv	Rz	Rc	Rt	Ra	<i>Rq</i>	Rsk	Rku
(μm)	(µm)	(µm)	(µm)	(µm)	(µm)	(μm)	(-)	(-)
38.2573	36.4542	74.7115	32.2891	141.754	10.7646	14.1629	-0.1383	3.2296

Note: Rp – maximum peak height, Rv – maximum valley depth, Rz – ten-point height, Rc – mean height of profile elements, Rt – total height of profile, Ra – arithmetical mean roughness, Rq – root mean square roughness, Rsk – skewness, Rku – kurtosis.



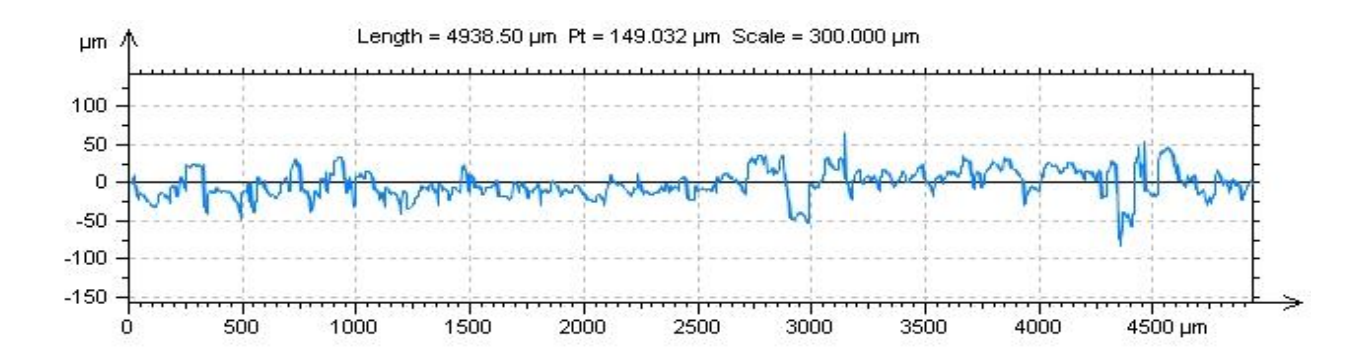


Figure 2 Surface profile measured parallel to the layer orientation (ISO 4287)

Table 3 Surface roughness parameters (ISO 4287) measured perpendicular to the layer orientation.

Rp	Rv	Rz	Rc	Rt	Ra	Rq	Rsk	Rku
(μm)	(µm)	(µm)	(µm)	(µm)	(µm)	(µm)	(-)	(-)
70.5174	52.7883	123.306	48.3985	123.306	25.6886	31.1927	0.6180	

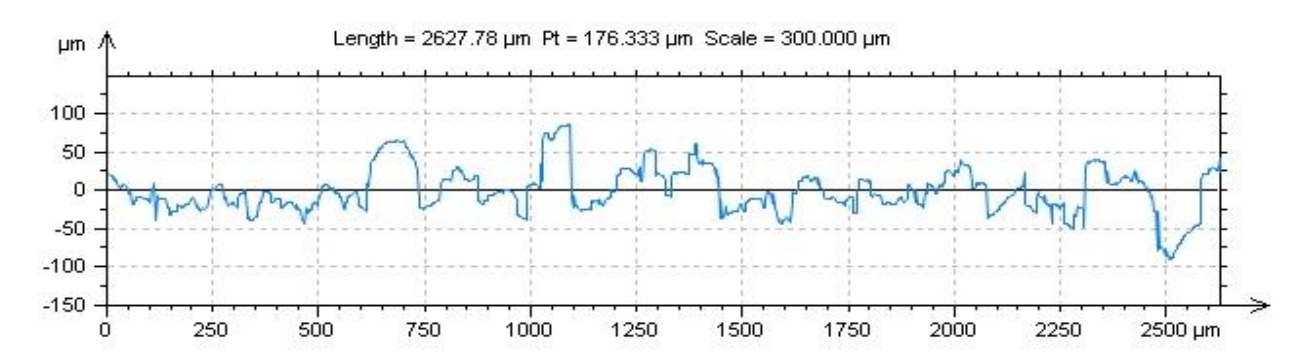


Figure 3 Surface profile measured perpendicular to the layer orientation (ISO 4287)

Table 4 Surface topography height parameters according to ISO 25178

S	<i>q</i> (μm)	Ssk (-)	Sku (-)	Sp (µm)	Sv (µm)	Sz (µm)	Sa (µm)
	24.5901	0.1283	3.4181	154.085	96.4152	250.501	19.3626

Sq – root mean square height, Ssk – skewness of the surface, Sku – kurtosis of the surface, Sp – maximum peak height, Sv – maximum pit depth, Sz – maximum height of the surface (Sp + Sv), Sa – arithmetic mean height.

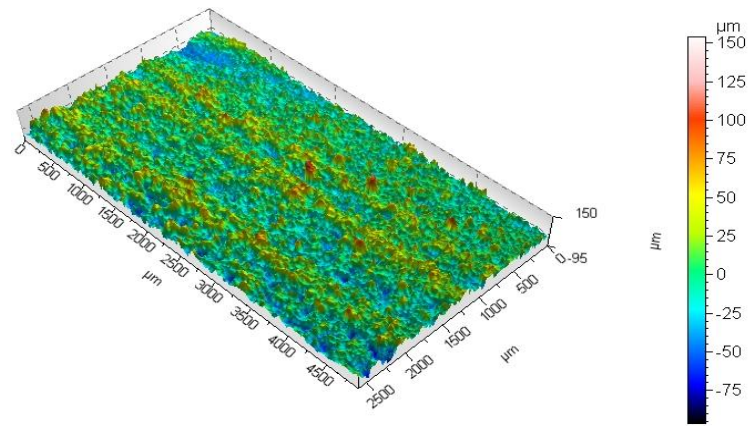


Figure 4 3D surface deviation map of roughness profile



Surface roughness was evaluated in two directions: parallel and perpendicular to the layer-building orientation. For the parallel direction, the average roughness Ra was 10.76 µm, and the total profile height Rt reached 141.75 µm. In contrast, for the perpendicular direction, Ra was 25.69 µm and Rt was 123.31 µm. These results indicate that measurement orientation has a significant effect on roughness values, consistent with findings in the literature, where differences in Ra up to 50% have been observed depending on direction [11]. The areal surface roughness, assessed according to ISO 25178, showed a Sa value of 15.3 µm, indicating a moderately rough surface. These results align with studies focused on SLM-produced zinc alloys, where Sa typically ranges between 12 and 18 µm [6]. Surface roughness also plays a key role in the degradation behavior of biodegradable implants. Increased roughness accelerates degradation, which may be undesirable for applications requiring slower resorption. One study demonstrated that implants with low Ra values (~2 µm) exhibited significantly slower degradation compared to those exceeding 10 µm [8,12].

The results of the average mass, volume, and experimentally determined density of ten 3D printed samples from the Zn0.4Mg0.4Ca alloy are summarized in **Table 5**. The average density calculated from these values was 7.2993 g/cm³, with a low standard deviation, indicating high consistency in the manufacturing process and structural homogeneity across the samples. This measured density exceeds the theoretical density of 6.97 g/cm³, which was calculated using the rule of mixtures based on the known weight fractions and densities of the individual elements Zn (7.14 g/cm³), Mg (1.74 g/cm³), and Ca (1.55 g/cm³). The difference suggests the presence of mechanisms beyond ideal solid-solution behavior. One possible explanation for the increased density is the formation of intermetallic phases with higher local density, such as Mg₂Zn₁₁ or CaZn₁₃, which may form during the solidification and elemental segregation that occurs in the selective laser melting process [3]. Such phases were also reported in studies of mechanically alloyed Zn–Mg–Ca systems, where they contributed to structural strengthening and increased bulk density [10]. Another contributing factor could be the high structural compaction achieved through rapid solidification typical for SLM. This process promotes the formation of a fine-grained, densely packed microstructure, which may slightly elevate the apparent bulk density compared to ideal theoretical predictions. Similar effects have been observed in other SLM-produced alloys [13,14].

Table 5 Overview of density measurements and theoretical comparison

Sample mass (g)	Sample volume (cm³)	Sample density (g/cm³)	Standard deviation (g/cm³)	Theoretical volume (g/cm³)	
1.0135	0.1389	7.2993	0.0379	6.97	

4. CONCLUSIONS

This study represents the initial phase of a broader research project aimed at evaluating the applicability of the Zn0.4Mg0.4Ca alloy in the additive manufacturing of biodegradable implants. The main objective was to verify whether this alloy can be successfully processed using Selective Laser Melting (SLM) and to assess its fundamental material properties. The experimental results confirmed good printability and favorable characteristics of the printed samples. The average microhardness reached 115.2 HV1, which represents a significant improvement over pure zinc and suggests the influence of alloying elements and the possible formation of strengthening intermetallic phases. Surface roughness was strongly affected by the orientation of the printed layers – in the direction parallel to the layers, the average Ra value was 10.76 μ m, while in the perpendicular direction it reached 25.69 μ m. Such surface irregularities may influence the corrosion behavior and biological response of the material, and therefore appropriate post-processing will be required to reduce roughness in future development. The measured density was 7.30 g/cm³, exceeding the theoretical value of 6.97 g/cm³, which indicates a high level of compaction and low porosity in printed material.

Based on these findings, the Zn0.4Mg0.4Ca alloy demonstrates promising potential for use in temporary biodegradable implant applications, particularly due to its increased hardness, sufficient density, and the



possibility of further surface optimization. However, this work represents only the first step. The next stage of the research will focus on printing a specific type of implant, the selection of which will be addressed in a separate study. We will then analyze the behavior of the alloy in a more complex geometry and evaluate its mechanical, microstructural, and biocompatibility properties in order to comprehensively assess its clinical potential.

ACKNOWLEDGEMENTS

This work was supported by the Scientific Grant Agency of The Ministry of Education of the Slovak republic No. VEGA 1/0408/23.

REFERENCES

- [1] BOWEN, P.K., DRELICH, J.W., GOLDMAN, J. Zinc exhibits ideal physiological corrosion behavior for bioabsorbable stents. *Advanced Materials*. 2016, vol. 28, no. 33, pp. 6117–6122.
- [2] KONG, L., HEYDARI, Z., LAMI, G.H., SABERI, A., BALTATU, M.S. A comprehensive review of the current research status of biodegradable zinc alloys and composites for biomedical applications. *Materials*. 2023.
- [3] LI, H., et al. Development of Zn-reinforced Mg matrix composites via high energy ball milling and sintering. *Coatings*. 2023, vol. 15, no. 5, p. 561. https://www.mdpi.com/2079-6412/15/5/561.
- [4] ZHU, D., et al. Alloying design of biodegradable zinc as promising bone implants. *Nature Communications*. 2019, vol. 10, p. 4156.
- [5] YANG, H., et al. Evolution of the degradation mechanism of pure zinc stent in the one-year study of rabbit abdominal aorta model. *Biomaterials*. 2017, vol. 145, pp. 92–105.
- [6] YASA, E., et al. Evaluation of surface roughness and defect formation after the selective laser melting process. *Materials*. 2020, vol. 13, no. 9, p. 1615.
- [7] GRYC, K., STROUHALOVA, M., SMETANA, B., SOCHA, L., MICHALEK, K. Influence of direct thermal analysis experimental conditions on determination of the high temperature phase transformation temperatures. *Archives of Metallurgy and Materials*. 2015, vol. 60, no. 4, pp. 2867–2871.
- [8] KOPP, A., et al. Influence of surface condition on the degradation behaviour and biocompatibility of additively manufactured magnesium scaffolds. Materials Science and Engineering: C, 2021, vol. 120, p. 111717.
- [9] MAMRILLA, W. *Characteristic of biodegradable alloy Zn–Mg–Ca for implants*. Košice. Dissertation, Technical University of Košice, 2023. In Slovak.
- [10] ZHANG, Y., et al. Advanced zinc–magnesium alloys prepared by mechanical alloying. *Metals*. 2022, vol. 12, no. 9, p. 1500. https://www.ncbi.nlm.nih.gov/pmc/articles/PMC9369638/.
- [11] KRUTH, J.P., et al. Surface quality improvement by parameters analysis, optimization and manufacturing process selection. *CIRP Journal of Manufacturing Science and Technology*. 2008, no. 1, pp. 20–25.
- [12] WONG, P.-C., et al. Relationship between the surface roughness of biodegradable Mg-based bulk metallic glass and the osteogenetic ability of MG63 osteoblast-like cells. *Materials*. 2020, vol. 13, no. 5, p. 1188.
- [13] MARKULIK, Š., et al. Production process optimization by reducing downtime and minimization of costs. In: *Advances in Physical, Social and Occupational Ergonomics (AHFE 2021)*. Cham: Springer, 2021, pp. 220–227.
- [14] GUAN, K., et al. A review of SLMed magnesium alloys: Processing, properties, and applications. *Metals*. 2020, vol. 10, no. 8, p. 1073.